Coating Individual Single-Walled Carbon Nanotubes with Nylon 6,10 through Emulsion Polymerization

Wei-Chiang Chen,[†] Randy K. Wang,[†] and Kirk J. Ziegler*[,†,‡,§]

Department of Chemical Engineering, Department of Materials Science and Engineering, and Center for Surface Science and Engineering, University of Florida, Gainesville, Florida 32611

ABSTRACT Solvent microenvironments are formed around individual single-walled carbon nanotubes (SWNTs) by mixing SWNT suspensions with water-immiscible organic solvents. These microenvironments are used to encapsulate the SWNTs with the monomer sebacoyl chloride. Hexamethylene diamine is then injected into the aqueous phase so the formation of nylon 6,10 is restricted to the interface between the microenvironment and water. This emulsion polymerization process results in uniform coatings of nylon 6,10 around individual SWNTs. The nylon-coated SWNTs remain dispersed in the aqueous phase and are highly luminescent at pH values ranging from 3 to 12. This emulsion polymerization method provides a general approach to coat nanotubes with various polymers.

KEYWORDS: carbon nanotubes • emulsion polymerization • nylon • microreactor • encapsulate

INTRODUCTION

Single-walled carbon nanotubes (SWNTs) have attracted much attention because of their mechanical strength, chemical inertness, and electronic properties (1−3). These properties make them ideal components for many applications including field effect transistors, sensors, and high strength composites. The tendency of nanotubes to aggregate into bundles makes dispersion important to many of these SWNT applications (4), especially in the preparation of composites (3, 5−11). Numerous covalent functionalization schemes have been developed to disperse nanotubes (12–14). However, the covalent functionalization of SWNTs destroys the advantageous electrical, optical, and mechanical properties. For this reason, surfactants are often used to stabilize aqueous SWNT suspensions. The anionic surfactants sodium dodecyl sulfate (SDS) and sodium dodecylbenzene sulfonate (SDBS) are frequently used because of the high dispersion quality and near-infrared (NIR) fluorescence properties (15−17).

Although surfactants preserve the inherent SWNT properties, the dispersion stability and fluorescence emission of SWNTs can be sensitive to extrinsic effects, including the state of aggregation (18−21), polarizability of the surrounding environment (22, 23), pH of the suspension (24, 25), sidewall defects (19, 25−28) and surfactant inhomogeneties (19, 27−29). These changes in dispersion and fluorescence can be used to monitor reactions (25, 30, 31) or sense chemical components (32). However, in many applications, these extrinsic factors limit the use of SWNTs, including biomedical applications where the pH and salt concentration in cells may influence the dispersion stability and fluorescence emission (33).

Some researchers already have developed processes to control the surfactant structure around SWNTs. We recently demonstrated that organic solvents (23) and shear (34) can alter the surfactant shell around SWNTs. These processes "anneal" the surfactant layer, providing better dispersion and protection to quenching mechanisms. Kim et al. encapsulated SWNTs by using surfactants with polymerizable counterions and a free radical initiator (35). Duque et al. utilized the surfactant surrounding SWNTs to create polymer−surfactant complexes that maintained the fluorescent properties of SWNTs even in acidic environments (24). Both of these studies demonstrated the ability to resuspend the polymer-coated SWNTs after freeze-drying. These initial approaches to control the surfactant structure show improvement to the dispersion and fluorescence properties across a range of conditions; however, the methods can not be generally applied to all polymer coatings.

In this study, a general method is developed for coating SWNTs with polymer using emulsion-like microenvironments surrounding SWNTs. Nylon 6,10 is chosen as a model system for in situ emulsion polymerization. The reaction occurs at the surface of the nanotube, providing a thin polymer coating around individual SWNTs. Fourier transform infrared spectroscopy (FT-IR) confirms the synthesis of nylon while AFM and fluorescence spectroscopy confirms that polymerization occurs on the surface of the SWNTs. Fluorescence, absorbance, and Raman spectra show that nylon is noncovalently bound to the nanotube without affecting either the dispersion or fluorescent properties of SWNTs. Further, these polymer coatings are shown to not

only provide an adequate barrier to the quenching effects of acid but also aid the redispersion of individual SWNTs in water.

EXPERIMENTAL SECTION

Preparation of Aqueous SWNT Suspensions. Aqueous SWNT suspensions were prepared with a given initial mass (40 mg) of raw SWNTs (Rice HPR 122.1) and mixed with 200 mL of aqueous sodium dodecyl benzene sulfonate (SDBS) (Sigma-Aldrich) surfactant solution (1 wt %). High-shear homogenization (IKA T-25 Ultra-Turrax) at 12 000 rpm for 2 h and ultra-sonication (Misonix S3000) with 90 % amplitude for 10 min were used to aid dispersion. After ultrasonication, the SWNT suspension was ultracentrifuged at 20 000 rpm (Beckman Coulter Optima L-90 K) for 3 h to remove nanotube bundles. The final concentration of suspended SWNTs is estimated to be 20 mg/L.

Interfacial Polymerization by Swelling Surfactant Micelles. A sebacoyl chloride (Sigma-Aldrich, 98 %) solution was prepared (0.5 M) in carbon tetrachloride (Sigma-Aldrich, 99 %). The aqueous SDBS-SWNT suspension (5 mL) was then added slowly to the sebacoyl chloride solution (5 mL). The mixture was shaken vigorously with a Vortex stirrer at 2000 rpm for 30 s to form the solvent-swelled microenvironments around SWNTs (23). The aqueous SWNT suspension was carefully removed from the bulk carbon tetrachloride after phase separation (approximately 1 h) with a glass pipet to prevent shearing and further emulsification. Hexamethylene diamine (Sigma-Aldrich, 97 %) was liquefied at 50 °C prior to injection. Liquid hexamethylene diamine (0.002 mL) was then added directly into the solvent-swelled aqueous SWNT suspension. After hexamethylene diamine was injected into the aqueous SWNT suspension, the color of the SWNT suspension gradually changed from black to bluish-gray during the formation of the nylon coating.

Resuspension. Dry powder samples of SDBS-SWNTs and polymer-coated SWNTs were obtained by freeze-drying (LAB-CONCO Freeze-Dryer 8). The SWNTs were redispersed by adding DI water (5 mL) to each powder sample and tip soni-cating (Misonix S3000) with 10 % amplitude for 1 min.

Characterization. NIR-fluorescence and vis-NIR absorbance spectra of all aqueous SWNT suspensions were characterized with an Applied NanoFluorescence Nanospectrolyzer (Houston, TX) with excitation from 662 and 784 nm diode lasers. Raman spectra of the aqueous SWNT suspensions and the solid powders of SWNTs before and after polymerization were recorded with a Renishaw Invia Bio Raman with a 785 nm diode laser source. All Raman spectra were normalized to the G-band ($\sim 1590 \ cm^{-1}$). The SDBS-SWNT and polymer-coated SWNT suspensions were also spin-coated onto fresh mica to collect tapping-mode AFM images on a Digital Instruments Dimension 3100. The diameters of SDBS-coated and nylon-coated SWNTs were measured from 10 AFM images of each sample with the NanoScope v5.30r1 software. At least 125 SWNTs were measured for each sample to generate the histograms.

The surfactant was removed for FT-IR analysis by adding ethyl acetate (5 mL) to the polymer-coated SWNT suspension. The mixture was then shaken with a Vortex stirrer at 2000 rpm for 30 s to remove the SDBS surfactant. After phase separation, the bulk ethyl acetate solution was removed and the polymer-coated SWNT suspension was freeze-dried, yielding a dry gray powder of polymer-coated SWNTs. The chemical structure of the polymer-coated SWNTs was analyzed by FT-IR spectroscopy (Nicolet MAGNA 760 FTIR).

RESULT AND DISCUSSION

The basis for the emulsion polymerization reaction is shown in Figure 1. Previously, we showed that mixing
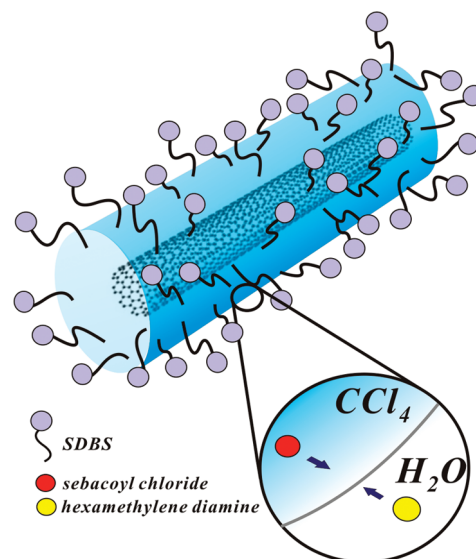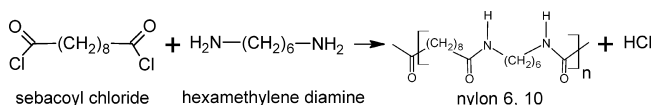

FIGURE 1. Mechanism for coating individual SWNTs with nylon via solvent microenvironments around the nanotube. Note that the image is not drawn to scale.

Scheme 1. Reaction of Sebacoyl Chloride with Hexamethylene Diamine To Form Nylon 6,10

aqueous SWNT suspensions with immiscible organic solvents changes the environment around the SWNT, resembling an emulsion-like microenvironment around the nanotube (23, 36). These solvent-swelled systems provide a controlled microreactor around the nanotube to conduct emulsion polymerization. Nylon 6,10 forms instantly from the condensation reaction of the two monomers: sebacoyl chloride and hexamethylene diamine, as shown in reaction Scheme 1. These two monomers can be dispersed separately in oil and water phases so the reaction is limited to the interface near the nanotube sidewall. The organic solvent containing the monomer sebacoyl chloride surrounds the nanotube by mixing the aqueous SDBS-SWNT suspension with carbon tetrachloride. The excess organic solvent is removed to prevent bulk interfacial polymerization. The monomer hexamethylene diamine is then added to the aqueous suspension to allow the polymerization reaction to occur at the interface near the nanotube, resulting in a thin polymer-coating of nylon 6,10 around the SWNT.

The first step in the encapsulation of SWNTs with nylon 6,10 is to bring sebacoyl chloride in close proximity to the nanotube sidewall. Figure 2a shows well-resolved fluorescence spectra characteristic of the initial SDBS-SWNT suspension. The fluorescence emission of SDBS-suspensions slightly blue-shifts (see the (7,5) and (7,6) SWNTs) and shows an increase in intensity when mixed with pure carbon tetrachloride. These spectral changes are associated with the formation of an emulsion-like microenvironment around the nanotube (23, 36). The blue-shift represents a change to a less polar environment, whereas the intensity increase could be due to either solvent effects (36) or reorganization of the
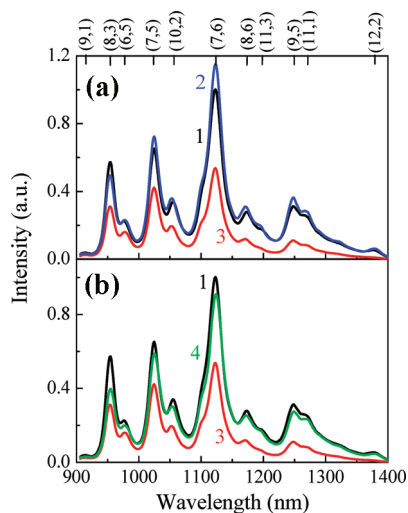
FIGURE 2. (a) Fluorescence spectra (Ex. = 662 nm) of the initial SDBS-coated SWNTs (*1*) and SDBS−SWNTs mixed with only carbon tetrachloride (*2*) or carbon tetrachloride containing sebacoyl chloride (*3*). (b) Fluorescence spectra (Ex. = 662 nm) of SWNTs before (*3*) and after 5 min of polymerization (*4*) compared to the initial SDBS−SWNT suspension (*1*).

FIGURE 3. (a) Raw and (b) background-corrected absorbance spectra of SDBS-coated SWNTs (*1*), SDBS-coated SWNTs mixed with carbon tetrachloride containing sebacoyl chloride (*2*), and nylon-coated SWNTs (*3*).

FIGURE 4. Normalized Raman spectra of the (a) SWNT suspension and (b) solid SWNT powder before and after polymerization. The inset shows the SWNT RBMs of each sample.

surfactant that minimizes quenching (23, 34). On the other hand, mixing the initial SDBS−SWNT suspensions with 0.5 M sebacoyl chloride in carbon tetrachloride yields a significant decrease in the fluorescence intensity of all SWNT (*n,m*) types when compared to either the initial suspension or the solvent-swelled states. The larger diameter SWNTs appear to be more sensitive to the new microenvironment and show the largest decreases in intensity. Several research groups have also noticed the sensitivity of large diameter SWNTs to quenching mechanisms (23, 29, 34, 36). Interestingly, the peak positions are the same with or without sebacoyl chloride added. The similarity in peak position suggests the microenvironment around the nanotube is similar (i.e., carbon tetrachloride). Therefore, the intensity decrease is associated with the presence of the sebacoyl chloride within the emulsion-like phase surrounding the SWNT. The decrease in intensity could be from doping (37−39) but, regardless, the spectral changes confirm the presence of sebacoyl chloride surrounding the SWNTs.

The fluorescence changes observed after sebacoyl chloride addition are reversed once the monomer hexamethylene diamine is added. The most notable change observed in Figure 2b is the increase in fluorescence intensity. The intensity for nearly all (*n,m*) SWNT types has recovered to values that are nearly identical to the initial SDBS−SWNT suspension rather than the spectra for SWNTs encased in a carbon tetrachloride shell. These differences are likely due to pH changes caused from reaction Scheme 1, which are shown below to affect the fluorescence intensity. The spectra also show a red-shift of the spectra, indicating once again that the environment surrounding the nanotube has been altered. The change of the spectral properties is likely due to the consumption of the sebacoyl chloride during reaction with the hexamethylene diamine at the interface. Similar
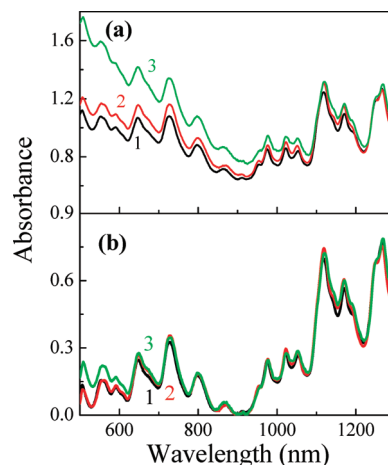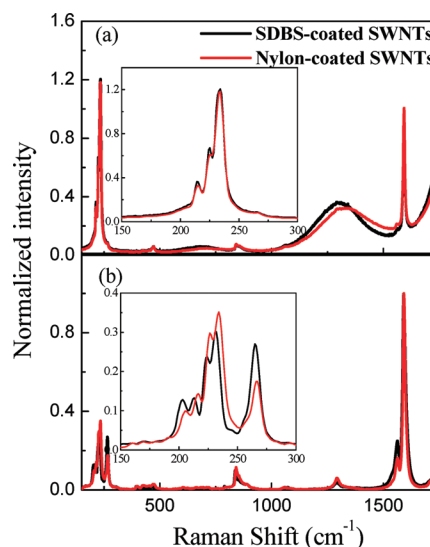
fluorescence spectral changes are also observed during the mixing and reaction phases when excited at 784 nm (not shown).

Although the red-shifts observed after the reaction could indicate that the nanotubes are aggregating during polymerization, both absorbance (Figure 3) and Raman (Figure 4) spectra do not indicate that aggregation occurs. Figure 3a shows the absorbance spectra of each SWNT suspension. The spectra have well-resolved peaks associated with the interband transitions of each (*n,m*) SWNT type. After the SWNT suspension is mixed with sebacoyl chloride, there is a slight red-shift and an increase in visible absorbance (400−900 nm). The nylon-coated SWNTs still have well-resolved peaks in the NIR region (900−1400 nm) but also show a further increase in visible absorbance. The higher absorbance background for the monomer- and polymer-coated SWNT suspensions seen in the visible light region is likely due to scattering from emulsions and polymer particles. After removing the effect of the background, which
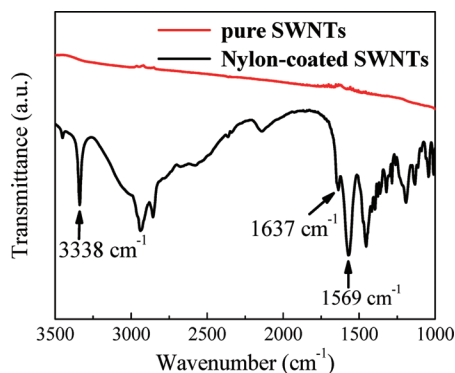
FIGURE 5. FTIR spectra of raw and nylon-coated SWNTs.

is shown in Figure 3b, the trend and intensity of the absorbance spectra are similar at each stage of the polymerization reaction. Therefore, the large polymer particles likely contain few nanotubes. The formation of the polymer particles could be reduced by controlling the amount of hexamethylene diamine injected.

The distinguishable and intense peaks in the NIR region indicate that SWNTs are individually suspended throughout the reaction. This conclusion is also supported by both liquid-phase and solid-state Raman spectra shown in Figure 4. The SWNT radial breathing modes (RBMs) of the liquid-phase Raman spectra in the inset of Figure 4a show no changes after polymerization to the so-called aggregation peak located at ~270 cm^{-1} (40). In addition, the solid-state Raman spectra shown in Figure 4b have an upshift of approximately 2−3 cm^{-1} in the RBMs. These upshifts have been observed for SWNTs embedded in polymer matrices (41). Buisson et al. developed a model to relate the shift in the RBMs to the structure of the polymer around the SWNTs (42). Their model suggests that polymer coatings around SWNT bundles should show a more significant upshift of the RBMs than individually coated SWNTs. On the basis of this model, the effect of nylon coating on either bundled or individual SWNTs is estimated to be 41 and 13 cm^{-1}, respectively. Although the upshift observed in the RBMs of Figure 4b is less than either estimate, the low magnitude of the shift would suggest that nylon coats individual rather than bundled SWNTs.

Pure nylon 6, 10 synthesized via interfacial polymerization is a white powder with characteristic FT-IR stretches of the amide-I peak at 1640 cm^{-1}, the amide-II peak at 1545 cm^{-1}, the C−H stretch at 2860 and 2940 cm^{-1}, and the N−H stretch at 3330 cm^{-1} (43). Figure 5 shows the FT-IR spectra of raw SWNTs and polymer-coated SWNTs. The polymer-coated SWNTs show amide-I, amide-II, and N−H stretching groups at 1637, 1569, and 3338 cm^{-1}, respectively. Comparing the FT-IR spectra of raw SWNTs to the polymer-coated SWNTs provides evidence that nylon 6,10 is formed through the interfacial polymerization reaction.

An AFM image of individual SWNTs suspended in SDBS is illustrated in Figure 6a. The inset of Figure 6a shows the diameter distribution is narrow with an average diameter of 1.2 nm. Figure 6b shows the nanotubes after the nylon 6,10 polymerization reaction. Individual SWNTs are still
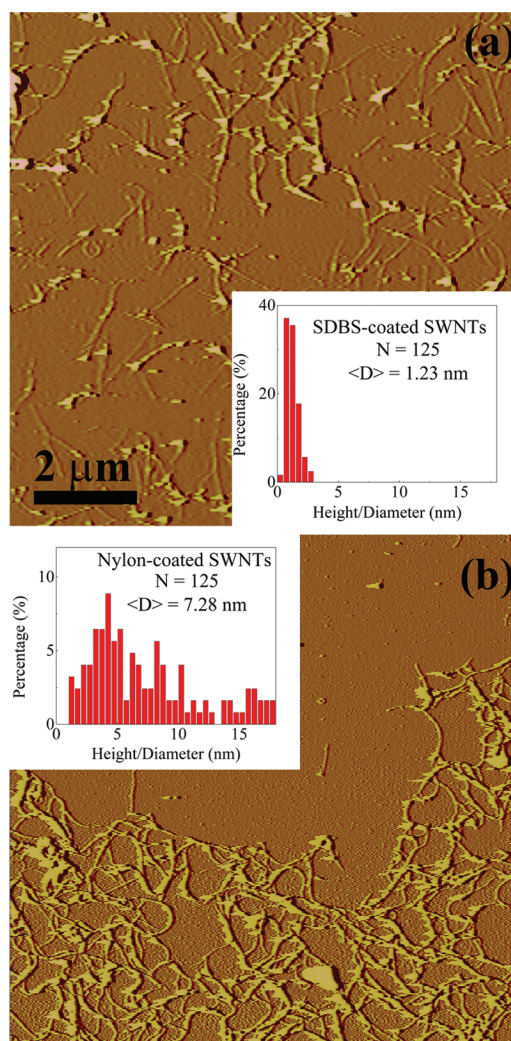

FIGURE 6. AFM images and corresponding histograms of diameter distribution for (a) SDBS-coated and (b) nylon-coated SWNT suspensions.

observed after the polymerization reaction; however, it is clear that the surface morphology has changed around the nanotube. After the polymerization reaction, the diameter distribution for nylon-coated SWNTs in the inset of Figure 6b becomes broader with an average diameter of 7.3 nm. The diameter distribution of the polymer-coated SWNTs suggests that the coating thickness ranges between 0.5 and 8 nm with an average thickness of 3 nm.

The thin coating of nylon encapsulating SWNTs should provide better protection to the fluorescence quenching effects of acid (24, 25, 29, 31, 44). The better protection from this layer was immediately obvious after polymerization because the fluorescence intensity was high (Figure 2b) despite the acidic pH generated from the reaction (Scheme 1). Figure 7 shows the effect of pH on the fluorescence intensity of different (*n,m*) SWNT types. The fluorescence intensity of all SWNT types in the initial suspension of SDBS-coated SWNTs steadily decrease as the pH is lowered from basic to acidic conditions, as observed by others (24, 25, 29, 31, 44). However, the fluorescence intensity of nylon-coated SWNTs is generally higher and more stable than the fluorescence of SDBS-coated SWNTs, especially for large diam-
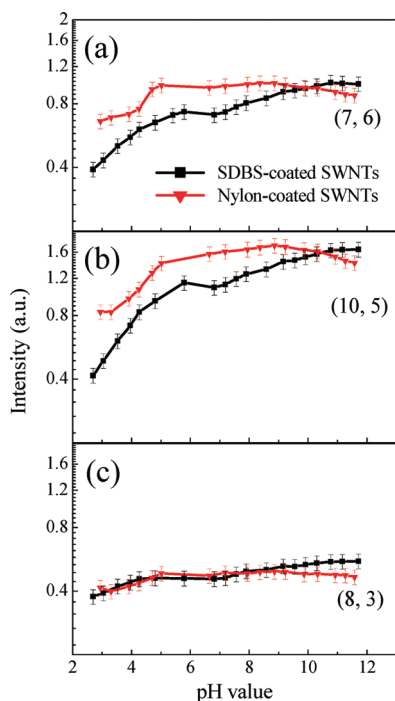
FIGURE 7. Effect of pH on the fluorescence intensity of the (a) (7,6) SWNT (Ex. = 662 nm), (b) (10,5) SWNT (Ex. = 784 nm), and (c) (8,3) SWNT (Ex. = 784 nm) types in SDBS- and nylon-coated SWNT suspensions.

FIGURE 8. Nylon-coated SWNTs are (a) freeze-dried and (b) redispersed in water. (c) Fluorescence spectra (Ex. = 662 nm) of nylon-coated SWNT before (*1*) and after (*2*) freeze-drying compared to SDBS-coated SWNTs redispersed in water after freeze-drying (*3*).

eter SWNTs. For example, the (10,5) SWNT type typically has an emission intensity that is 50−100 % higher than the SDBS-coated SWNTs at acidic pH. The (7,6) SWNT type also has significant improvement across the acidic pH region, whereas the (8,3) SWNT type has little improvement to the emission intensity. The lack of any changes for the (8,3) SWNT type likely indicates that the initial surfactant structure provides a nearly ideal protective layer to pH quenching, minimizing any benefit achieved by adding a nylon coating.

The nylon coating around SWNTs also helps to redisperse the nanotubes in water. Images a and b in Figure 8 show nylon-coated SWNTs after being freeze-dried and resuspended, respectively. The nylon-coated SWNTs are redispersed in water without any visible aggregation and the fluorescence spectrum in Figure 8c shows well-resolved peaks. The fluorescence intensity is less than half the initial intensity; however, the nylon-coated SWNTs have four times higher fluorescence intensity than freeze-dried SWNTs coated with only SDBS.

An important feature of coating SWNTs through this interfacial polymerization reaction is that the nylon coating surrounding the nanotubes does not affect the optical properties of the SWNTs. The solid state Raman spectra shown in Figure 4b shows no changes after polymerization to the D-band ($\sim$1290 cm^{-1}) associated with covalent bonding to the nanotube sidewall. These results are in agreement with the intense fluorescence spectra seen in Figure 2b, which is very sensitive to sidewall reactions (25). Therefore, the polymer coating appears to be physisorbed onto the SWNT sidewall, allowing the structure and properties of SWNTs to be preserved.
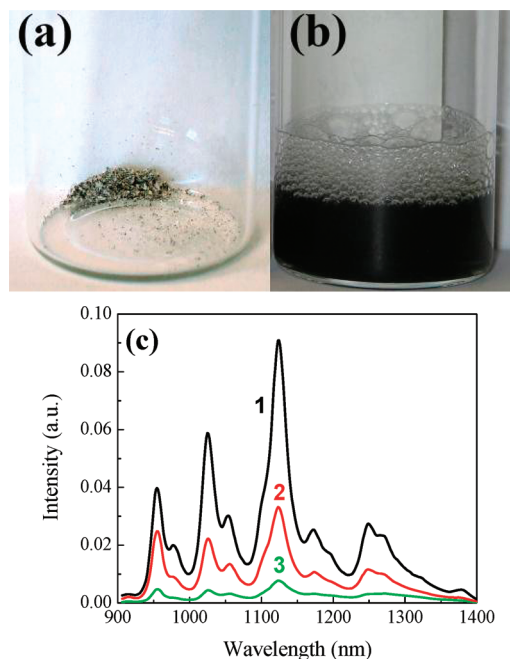
CONCLUSIONS

Nylon 6,10 is noncovalently coated around individual SWNTs by interfacial polymerization in solvent microenvironments that encase individual nanotubes. These nylon-coated SWNTs are still well-dispersed in the aqueous phase without any indication of aggregation based on Raman and fluorescence spectroscopy. The nylon-coated SWNTs are easily redispersed in water after freeze-drying. The fluorescence intensity of the nylon-coated SWNTs remains high at both acidic and basic pH conditions. The generality of the interfacial polymerization approach enables the synthesis of many different polymer coatings around nanotubes.

REFERENCES AND NOTES
(1) Moniruzzaman, M.; Winey, K. I. *Macromolecules* **2006**, *39* (16), 5194–5205.
(2) Endo, M.; Hayashi, T.; Kim, Y. A.; Terrones, M.; Dresselhaus, M. S. *Philos. Trans. R. Soc. London, Ser. A* **2004**, *362* (1823), 2223–2238.
(3) Ajayan, P. M.; Tour, J. M. *Nature* **2007**, *447*, 1066–1068.
(4) Vaisman, L.; Wagner, H. D.; Marom, G. *Adv. Colloid Interface Sci.* **2006**, *128−130*, 37–46.
(5) Barraza, H. J.; Pompeo, F.; O'Rea, E. A.; Resasco, D. E. *Nano Lett.* **2002**, *2* (8), 797–802.
(6) Gao, J.; Itkis, M. E.; Yu, A.; Bekyarova, E.; Zhao, B.; Haddon, R. C. *J. Am. Chem. Soc.* **2005**, *127* (11), 3847–3854.
(7) Gao, J.; Zhao, B.; Itkis, M. E.; Bekyarova, E.; Hu, H.; Kranak, V.; Yu, A.; Haddon, R. C. *J. Am. Chem. Soc.* **2006**, *128* (23), 7492–7496.
(8) Haggenmueller, R.; Du, F.; Fischer, J. E.; Winey, K. I. *Polymer* **2006**, *47* (7), 2381–2388.
(9) Kang, M.; Myung, S. J.; Jin, H.-J. *Polymer* **2006**, *47* (11), 3961–3966.

(10) Kim, H.-S.; Park, B. H.; Yoon, J.-S.; Jin, H.-J. *Mater. Lett.* **2007**, *61* (11−12), 2251−2254.

(11) Moniruzzaman, M.; Chattopadhyay, J.; Billups, W. E.; Winey, K. I. *Nano Lett.* **2007**, *7* (5), 1178−1185.

(12) Bahr, J. L.; Tour, J. M. *J. Mater. Chem.* **2002**, *12* (7), 1952−1958.

(13) Hirsch, A. *Angew. Chem., Int. Ed.* **2002**, *41* (11), 1853−1859.

(14) Banerjee, S.; Hemraj-Benny, T.; Wong, S. S. *Adv. Mater.* **2005**, *17* (1), 17−29.

(15) Tan, Y.; Resasco, D. E. *J. Phys. Chem. B* **2005**, *109* (30), 14454.

(16) Moore, V. C.; Strano, M. S.; Haroz, E. H.; Hauge, R. H.; Smalley, R. E. *Nano Lett.* **2003**, *3* (10), 1379−1382.

(17) Haggenmueller, R.; Rahatekar, S. S.; Fagan, J. A.; Chun, J. H.; Becker, M. L.; Naik, R. R.; Krauss, T.; Carlson, L.; Kadla, J. F.; Trulove, P. C.; Fox, D. F.; DeLong, H. C.; Fang, Z. C.; Kelley, S. O.; Gilman, J. W. *Langmuir* **2008**, *24* (9), 5070.

(18) Crochet, J.; Clemens, M.; Hertel, T. *J. Am. Chem. Soc.* **2007**, *129* (26), 8058.

(19) Qian, H.; Georgi, C.; Anderson, N.; Green, A. A.; Hersam, M. C.; Novotny, L.; Hartschuh, A. *Nano Lett.* **2008**, *8*, 1363−1367.

(20) Tan, P. H.; Rozhin, A. G.; Hasan, T.; Hu, P.; Scardaci, V.; Milne, W. I.; Ferrari, A. C. *Phys. Rev. Lett.* **2007**, *99* (13), 137402-1− 137402-4.

(21) Torrens, O. N.; Milkie, D. E.; Zheng, M.; Kikkawa, J. M. *Nano Lett.* **2006**, *6* (12), 2864.

(22) Choi, J. H.; Strano, M. S. *Appl. Phys. Lett.* **2007**, *90*, 223114.

(23) Wang, R. K.; Chen, W.-C.; Campos, D. K.; Ziegler, K. J. *J. Am. Chem. Soc.* **2008**, *130* (48), 16330.

(24) Duque, J. G.; Cognet, L.; Parra-Vasquez, A. N. G.; Nicholas, N.; Schmidt, H. K.; Pasquali, M. *J. Am. Chem. Soc.* **2008**, *130*, 2626− 2633.

(25) Cognet, L.; Tsyboulski, D. A.; Rocha, J.-D. R.; Doyle, C. D.; Tour, J. M.; Weisman, R. B. *Science* **2007**, *316* (5830), 1465−1468.

(26) Lefebvre, J.; Austing, D. G.; Bond, J.; Finnie, P. *Nano Lett.* **2006**, *6* (8), 1603.

(27) Gokus, T.; Hartschuh, A.; Harutyunyan, H.; Allegrini, M.; Hennrich, F.; Kappes, M.; Green, A. A.; Hersam, M. C.; Araujo, P. T.; Jorio, A. *Appl. Phys. Lett.* **2008**, *92*, 153116.

(28) Tsyboulski, D. A.; Rocha, J. D. R.; Bachilo, S. M.; Cognet, L.; Weisman, R. B. *Nano Lett.* **2007**, *7* (10), 3080.

(29) Blackburn, J. L.; McDonald, T. J.; Metzger, W. K.; Engtrakul, C.; Rumbles, G.; Heben, M. J. *Nano Lett.* **2008**, *8*, 1047−1054.

(30) Doyle, C. D.; Rocha, J. D. R.; Weisman, R. B.; Tour, J. M. *J. Am. Chem. Soc.* **2008**, *130* (21), 6795.

(31) Dukovic, G.; White, B. E.; Zhou, Z. Y.; Wang, F.; Jockusch, S.; Steigerwald, M. L.; Heinz, T. F.; Friesner, R. A.; Turro, N. J.; Brus, L. E. *J. Am. Chem. Soc.* **2004**, *126*, 15269−15276.

(32) Endo, M.; Strano, M. S.; Ajayan, P. M. Potential Applications of Carbon Nanotubes. In *Carbon Nanotubes*; Jorio, A., Dresselhaus, G., Dresselhaus, M. S., Eds.; Springer-Verlag: Berlin, 2008; Vol. 111, pp 13−61.

(33) Niyogi, S.; Boukhalfa, S.; Chikkannanavar, S. B.; McDonald, T. J.; Heben, M. J.; Doorn, S. K. *J. Am. Chem. Soc.* **2007**, *129*, 1898− 1899.

(34) Silvera-Batista, C. A.; Weinberg, P.; Butler, J. E.; Ziegler, K. J. *J. Am. Chem. Soc.* **2009**, submitted.

(35) Kim, T. H.; Doe, C.; Kline, S. R.; Choi, S. M. *Adv. Mater.* **2007**, *19* (7), 929−933.

(36) Wang, R. K.; Silvera-Batista, C.; Weinberg, P.; Ziegler, K. J. **2009**, in preparation.

(37) Dresselhaus, M. S.; Eklund, P. C. *Adv. Phys.* **2000**, *49* (6), 705− 814.

(38) Moonoosawmy, K. R.; Kruse, P. *J. Am. Chem. Soc.* **2008**, *130*, 13417−13424.

(39) Zhou, W.; Vavro, J.; Nemes, N. M.; Fischer, J. E.; Borondics, F.; Kamaras, K.; Tanner, D. B. *Phys. Rev. B* **2005**, *71* (20), 205423.

(40) Heller, D. A.; Barone, P. W.; Swanson, J. P.; Mayrhofer, R. M.; Strano, M. S. *J. Phys. Chem. B* **2004**, *108* (22), 6905−6909.

(41) Lefrant, S. *Curr. Appl. Phys.* **2002**, *2* (6), 479−482.

(42) Buisson, J.-P.; Chauvet, O.; Lefrant, S.; Stephan, C.; Benoit, J.-M. *Mater. Res. Soc. Symp. Proc.* **2001**, *633*, A14.12.1.

(43) Kohan, M. I. *Nylon Plastics*; Wiley: New York, 1973.

(44) Strano, M. S.; Huffman, C. B.; Moore, V. C.; O'Connell, M. J.; Haroz, E. H.; Hubbard, J.; Miller, M.; Rialon, K.; Kittrell, C.; Ramash, S.; Hauge, R. H.; Smalley, R. E. *J. Phys. Chem. B* **2003**, *107*, 6979.